

## Flexible transparent conductive coatings by combining self-assembly with sintering of silver nanoparticles performed at room temperature

Michael Layani and Shlomo Magdassi\*

Received 8th July 2011, Accepted 27th July 2011

DOI: 10.1039/c1jm13174e

Transparent conductive coatings are essential for fabrication of a variety of printed electronic devices such as flexible displays and solar cells. We report on a simple method to obtain such coatings by using aqueous dispersions of silver nanoparticles in an evaporative lithography process which is performed directly onto plastic substrates. In essence, a droplet containing silver nanoparticles is placed on top of a metallic mesh, instantaneously spreading over the mesh and the plastic substrate, and after the flow of the dispersion towards the wires of the mesh and drying, a transparent grid composed of the nanoparticles is formed. The silver nanoparticles are tailored to self-sinter upon short exposure to HCl vapors, due to the presence of polyacrylic acid salt on the surface of the particles. Therefore, immediate sintering of the silver nanoparticles in the thin lines of the grid occurs even at room temperature, enabling formation of transparent, flexible conductive grid on heat-sensitive substrates. The process yielded a conductive array having a very low sheet resistance,  $9 \pm 0.8 \Omega/\square$ , and a transparency above 75%. The application of the flexible conductive grid, which can replace conventional and expensive ITO, is demonstrated in an electroluminescent (EL) device.

## Introduction

The current industrial demand for transparent and conductive coatings for printed electronics has led to various approaches for fabrication of such coatings.<sup>1,2</sup>

These approaches are mainly based on patterning methods and self-assembly of nanoparticles (NPs). For example, Kang and Guo used nano-imprinting lithography for fabrication of a gold transparent grid, by which the metal line thickness and the aperture ratio were varied, and demonstrated the use of the grid as the anode in an OLED device.<sup>3</sup> Recently we have shown how the printing of arrays of micrometer-sized rings composed of silver nanoparticles leads to the formation of a transparent and conductive grid.<sup>4</sup> The rings are formed due to the coffee stain effect,<sup>5</sup> where a droplet containing particles is pinned to the substrate and during evaporation of the liquid the particles are moved to the periphery of the droplet. Once the droplet is dried, a ring composed of closely packed nanoparticles is formed, while the width of the rim of the ring is below 5 micrometres, enabling the use of the ring pattern as a transparent conductive electrode. Although this method enables fabrication of conductive layers with high transparency, it has some inherent limitations: printing a large area would require a very accurate and environmentally controlled inkjet printer, special adjustment of the ink parameters is needed for each type of substrate, to meet the wetting and

evaporation behaviour that lead to ring formation, and finally, the printing process should be slow in order to avoid destruction of the rings.

The self-assembly of nanoparticles was also studied by Vakarelski *et al.* as a simple method for patterning of gold nanoparticles.<sup>6</sup> On top of a first layer composed of latex particles, they placed a droplet containing smaller gold NPs. The flux caused by evaporation forced the gold particles to assemble around the large latex particles. Once the droplet was fully evaporated, the latex layer was removed, and a small area, 0.5 mm<sup>2</sup>, of patterned gold NPs was obtained. This approach of evaporative lithography<sup>7,8</sup> was suggested by Vakarelski *et al.* as a method for fabrication of transparent and conductive coatings, which would require an additional step of sintering the nanoparticles.

Recently, Higashitani *et al.* have published<sup>9</sup> a novel fabrication method for obtaining transparent conductive films on plastic substrates using an evaporative lithography method. The fabrication is based on a three-step process: at first, a stainless-steel mesh is placed on top of a plasma-treated glass substrate. In the next step, a droplet containing gold NPs is placed on top of the mesh, instantaneously spreading over the mesh and the glass substrate. During evaporation, the liquid flows towards the metal wires of the mesh, leaving an empty area of the glass in each square of the mesh. After complete evaporation, the mesh is removed from the glass, and a transparent grid composed of the gold NPs is obtained. At this stage, the network was not conductive due to the presence of polymeric stabilizer around the

Casali Institute of Applied Chemistry, Institute of Chemistry and the Center for Nanoscience and Nanotechnology, The Hebrew University of Jerusalem, Jerusalem, 91904, Israel. E-mail: Magdassi@cc.huji.ac.il

particles. Hence, the polymers needed to burn out by heating the network on the glass at 425 °C for 20 min in order to make the particles directly contact each other. Then, the conductive network was transferred by pressing it into a thin layer of UV hardening resin coated on a PET film followed by UV radiation for 10 minutes.

Obviously, the need to sinter the particles at high temperatures prevents the possibility for obtaining the transparent grid directly on a plastic substrate, and requires a complicated transfer process of the grid from the glass to a soft film forming material.

In order to overcome these obstacles and to perform a similar process directly on heat-sensitive substrates, we combined the Higashitani *et al.* concept<sup>9</sup> with our recently reported method for obtaining conductive patterns from metallic nanoparticles while the sintering process is conducted at room temperature. The process is based on using silver dispersion in which the nanoparticles can undergo a sintering process without the need to burn out the organic stabilizer. The spontaneous sintering that occurs even at RT is based on interaction with a coagulating agent or replacing the stabilizer on the surface of the NP by a much smaller moiety. For example, this chemical sintering process can be triggered by using dispersion of silver nanoparticle with polyacrylic acid (PAA) as an electro-steric stabilizer on the particle surface, and bringing it into contact with a polycation, sodium chloride solution and even while exposed to HCl vapors.<sup>10,11</sup> In the case of using NaCl as the sintering triggering agent, it was found that the chloride ions replace the carboxylic anchoring groups of the dispersing agent, PAA, and enable the close contact between the particles which ends with immediate sintering of the nanoparticles, and therefore to electrical conductivity.

Therefore, implementation of the concept described by Higashitani for the PAA stabilized NP enabled us to form a transparent conductive coating directly on flexible plastic substrates and greatly simplify the fabrication process. The application of the flexible transparent conductive grid, which can replace the conventional and expensive ITO, is demonstrated in a plastic electroluminescent (EL) device.

## Experimental section

The synthesis of the silver NP dispersion (42 wt%) was performed as described by Magdassi *et al.*,<sup>11</sup> yielding nanoparticles which are stabilized by polyacrylic acid sodium salt ( $M_w$  8 kD), having an average size of  $14 \pm 3$  nm and a zeta potential of  $-42$  mV. Dispersions with various concentrations of the nanoparticles were made by diluting the concentrated dispersion with triple distilled water (TDW,  $0.55 \mu\text{S cm}^{-1}$ ).

Fabrication of the transparent grid was conducted directly on the plastic substrate, without any transfer and heat sintering processes. As shown schematically in Fig. 1, a stainless steel mesh was placed on a PET substrate, followed by addition of a 35 microlitre droplet of a silver dispersion with various silver contents. The liquid immediately wets the mesh, and after 5 minutes the stainless steel grid is removed, leaving a grid pattern on the plastic substrate. The PET substrate (Jolybar, Israel) and the stainless steel 420 mesh (a gift from Emmtech, Israel) were treated by plasma prior to their use (in 20% oxygen for 2 minutes,

PICO system, Deiner Electronics). The diameter of the mesh wires was 25 micrometres. Chemical sintering of the grids was performed at room temperature by exposing the PET with an Ag grid pattern to HCl vapors for 30 seconds. This was achieved by putting it in a 10 mL glass Petri dish, which was placed in a larger Petri dish (100 mL) containing 10 mL of conc. HCl (37 wt%, Aldrich).

The four-layer (PET:grid pattern:ZnS:BaTiO<sub>3</sub>) electroluminescent device was fabricated as follows: Ag grid patterns were fabricated on the PET by evaporative lithography, followed by chemical sintering, as described above. On top of the conductive grid, a layer of ZnS particles (MOBIChem Scientific Engineering, Israel) was coated by Dr Blade; after drying at 60 °C, this was coated with a double layer of barium titanate (MOBIChem Scientific Engineering, Israel). On top of the barium titanate, the non-transparent electrode of the device was achieved by inkjet printing of the silver dispersion (20 wt% Ag) containing 10 wt% propylene glycol and 0.05% of BYK 348 as wetting agents. The printing was performed by an Omnijet printer (Unijet, Korea) with 30 pL (Samsung) printheads, at 1000 Hz. The printed pattern was then sintered under HCl vapors, as described above.

The cross-sectional profiles of the lines were measured using a Veeco® Dektak 150 + Surface Profiler. The surface-tension measurements were carried out by a pendant drop tensiometer (First-Ten-Angstrom 32).

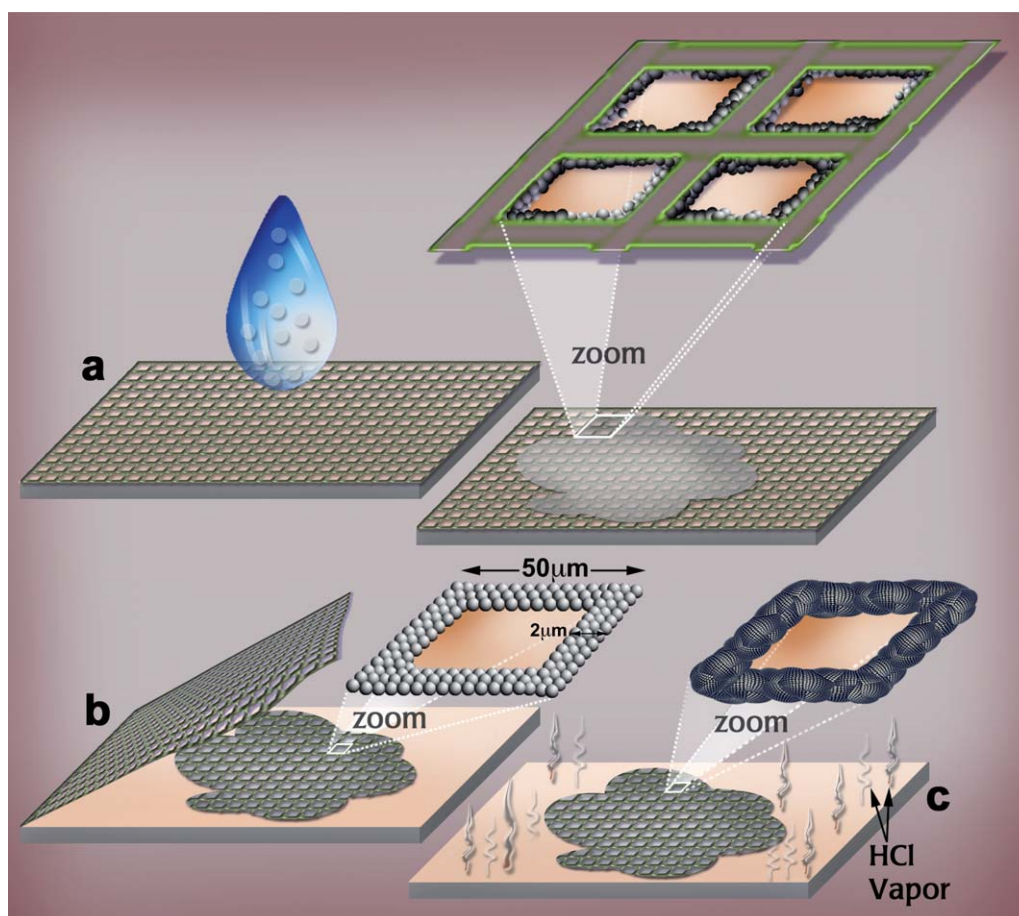
The grid patterns were imaged using an optical microscope and an HR-SEM microscope (Philips, Sirion HR-SEM).

The transparency and electric resistivity of the networks were measured at different points using a spectrometer (UV) and a four-pin probe surface resistivity meter, respectively, VARIAN carry 100 bio and Cascade Microtech Inc.

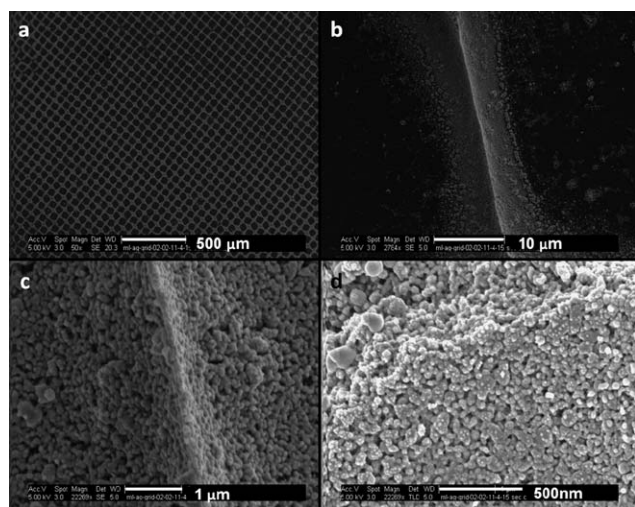
## Results and discussion

Fig. 2 shows HR-SEM images of the chemically sintered grid and line formed by using 8 wt% silver dispersion. It can be seen that the grid is composed of closely packed silver nanoparticles, which assemble in the form of a cone in each line of the grid. The line width is below 7 micrometres, much smaller than the dimensions of the stainless steel mesh (wire diameter, 25 micrometres), and this makes the whole grid transparent. This structure is probably due to the capillary forces that cause the upward movement of the dispersion at the gap between the metal wires and the plastic substrate. It should be noted that a 30  $\mu\text{L}$  droplet was sufficient to form a grid area of  $\sim 5$  sq cm. Once the nanoparticles are self-assembled into the grid, they should be sintered in order to have electrical conductivity. This is achieved by exposure to HCl vapors, which causes the removal of the polymeric stabilizer, PAA, from the particles' surface, by the chloride ions,<sup>11</sup> thus enabling a close contact between the particles.

The effect of the exposure to HCl vapors on the morphology of the silver nanoparticles is presented in Fig. 3; the cone form is not affected by the exposure to the vapors, but there is a significant increase in the silver particle size and formation of percolation paths due to the sintering of the nanoparticles, in agreement with our previous report.<sup>11</sup> Interestingly, in the previous work, we showed that the sintering by HCl vapours can be achieved for a height of about 200 nm, while here we found that the process



**Fig. 1** Schematic presentation of the fabrication process to obtain a transparent and conductive metallic grid.



**Fig. 2** SEM images of the transparent grid composed of silver NPs (formed using an 8 wt% silver nanoparticle dispersion): (a) a  $2 \times 2$  mm section of the sintered silver grid; (b–d): one line of the grid at various magnifications.

can take place at thicknesses as high as  $1.2 \mu\text{m}$ , probably due to the porosity of the obtained lines.

It should be noted that upon exposure to HCl vapor, the particles do not undergo a complete annealing process, and

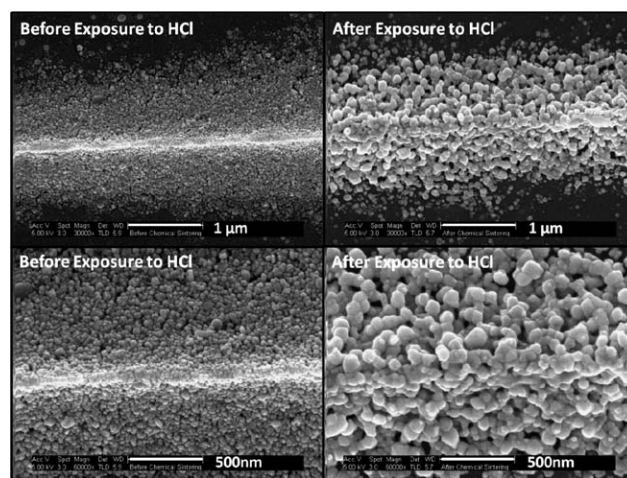


**Fig. 3** HR-SEM images of the grid lines before and after the chemical sintering, at different magnifications.

during sintering necks are formed between the particles. Thus, the formed line retains its general shape of a cone, but has a percolation path between the particles. The sintering process leads to formation of a conductive array having a low sheet resistance value of  $9 \pm 0.8 \Omega/\square$  ( $\sim 1^{-5} \Omega \text{ cm}$ ). Interestingly, the sheet is higher than that obtained by the coffee ring method, but it is still in the range of commercial ITO.



Fig. 4 shows a typical height profile of the sintered grid, in which the average height was  $1123 \pm 163$  nm. Most probably, the height differences are caused by the different gap distances between the mesh and the substrate. The average width at the base of the cone is  $5.7 \pm 1.3$   $\mu\text{m}$ . These very narrow lines led to high transparency,  $77 \pm 5\%$ , as demonstrated in Fig. 6d.

It should be noted that the sheet resistance and transparency did not change after storage of the sintered grid for at least 2 months at room temperature. Also, the transparency values did not change before and after exposure to the vapors.

Interestingly, the average height of the silver lines in our system is about 10 times higher than that obtained by Higashitani<sup>9</sup> *et al.* using gold nanoparticles of similar size. The main differences between the two systems (besides having gold and silver) are the different substrates (glass and PET) and the much larger concentration of nanoparticles in our system (8 wt% compared to 2 wt%). Since the PET substrate is treated by plasma and the contact angle of water is similar to that of the glass (below  $5^\circ$ ), it is most likely that the dominant parameter is the concentration of the particles in the dispersion. Indeed, while evaluating the dependence of line height on the concentration of the silver in the dispersion (Fig. 5a), it was found that the larger the concentration of silver the greater the line height.

This finding is important, since achieving a high aspect ratio of the conductive lines is advantageous in a variety of applications, such as solar cells<sup>12</sup> and OLED devices. However, as shown in Fig. 5a, above 10 wt% silver this dependency levels off. In addition, the line width also increases with the increase in metal load of the dispersion; at 20 wt% silver, the line thickness is about 25 microns, which causes the transparency of the grid to decrease to about 40%. It should be noted that increasing the metal load of the dispersion changes the viscosity from  $\sim 7$  cP in 10% metal load to 18 cP in 40% metal load. These changes in viscosity might affect the capillary movement of the particles. By comparing Fig. 5a and b, it seems that the height is strongly dependent on the metal load at the low concentrations, while the width is strongly dependent on the metal load at the high concentrations. It should be mentioned that at low metal load (0.5 wt%), the silver NP formed grids; however, they were composed of separated lines rather than a continuous grid. This problem of disconnected lines occurred up to 5 wt% metal load, so conductive grids can be obtained by this method only at higher metal load. From an application point of view, these different effects of the metal load in the dispersion would require a tradeoff between conductivity and transparency through the control of dispersion properties.

The applicability of the transparent conductive grid is demonstrated in a plastic EL device (Fig. 6), for which all

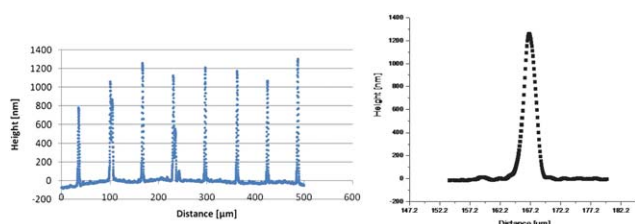


Fig. 4 Typical height profile of Ag grid lines.

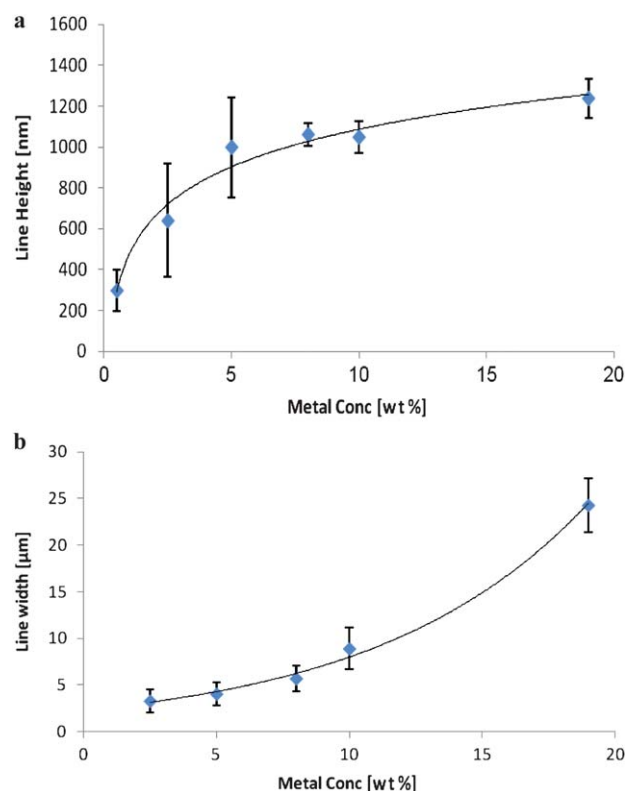


Fig. 5 (a) Average height of lines as a function of metal concentration. (b) Average line width as a function of metal concentration.

transparent electrode preparation steps were conducted at room temperature. Fig. 6a shows the HU symbol, observed by applying 110 volts between the transparent grid and the inkjet printed pattern. It should be noted that the whole fabrication process took less than 30 minutes, largely due to the use of the rapid sintering technique. Qualitatively, we have not seen any difference in performance of the EL device after exposure of both bottom and transparent electrodes to HCl vapour.

It should be noted that qualitative bending experiments show that the EL remained functional even after bending the substrate

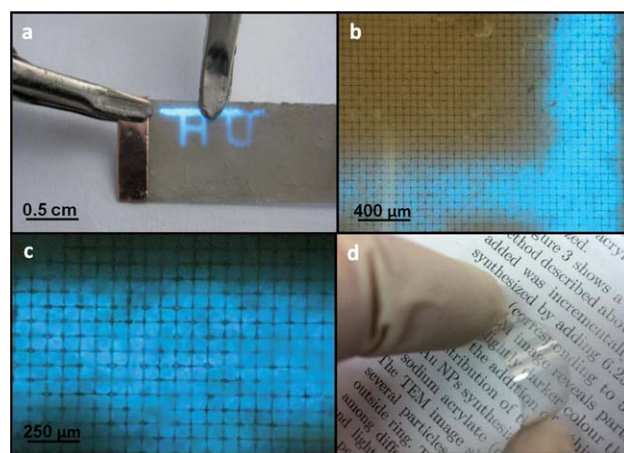


Fig. 6 (a-c) Electroluminescent device picture with a bias of 110 V at different magnifications. (d) Demonstration of the flexibility and transparency of the conductive silver grid.

at angles below about 20°, showing that the arrays may be suitable for applications in which flexibility is required.

Adhesion of the grid was tested by a tape test and by immersing the grid in water. It was found that the tape test caused failure of some parts of the grid, and if the samples were immersed in water for a prolonged time the patterns start to dissolve. In order to overcome this problem, we found that if the grids are heated at 130 °C for 10 minutes, the durability of the patterns improved significantly in both tape and immersion tests. As known in plastic electronics, such heat post-treatment is acceptable for many plastic substrates. It should be noted that the heat treatment is performed after the particles were sintered at room temperature, and that this heat treatment is not sufficient by itself to cause sintering of the silver nanoparticles used in this study.

## Conclusions

In conclusion, we have shown a simple process for fabricating conductive and transparent electrodes on plastic substrates. The process is based on direct patterning of silver nanoparticles on a PET substrate, while the sintering process is conducted at room temperature. The sintering is achieved rapidly at room temperature by using nanoparticles stabilized by polyacrylic acid salt, upon contact with HCl vapors. This makes the process suitable for a variety of heat-sensitive plastic substrates and may open new applications based on low cost substrates.

## Acknowledgements

This research was partly supported by the European Community's Seventh Framework Program, through LOTUS Project (no. 248816), and by the SES Magnet Program of the Israel Trade and Industry Ministry.

## Notes and references

- 1 D. S. Hecht, L. B. Hu and G. Irvin, *Adv. Mater.*, 2011, **23**, 1482–1513.
- 2 A. Kumar and C. W. Zhou, *ACS Nano*, 2010, **4**, 11–14.
- 3 M. G. Kang and L. J. Guo, *Adv. Mater.*, 2007, **19**, 1391–1396.
- 4 M. Layani, M. Gruchko, O. Milo, I. Balberg, D. Azulay and S. Magdassi, *ACS Nano*, 2009, **3**, 3537–3542.
- 5 R. D. Deegan, O. Bakajin, T. F. Dupont, G. Huber, S. R. Nagel and T. A. Witten, *Nature*, 1997, **389**, 827–829.
- 6 I. U. Vakarelski, D. Y. C. Chan, T. Nonoguchi, H. Shinto and K. Higashitani, *Phys. Rev. Lett.*, 2009, **102**, 0583031–0583034.
- 7 D. J. Harris and J. A. Lewis, *Langmuir*, 2008, **24**, 3681–3685.
- 8 D. J. Harris, H. Hu, J. C. Conrad and J. A. Lewis, *Phys. Rev. Lett.*, 2007, **98**, 1483011–1483014.
- 9 K. Higashitani, C. E. McNamee and M. Nakayama, *Langmuir*, 2011, 2080–2083.
- 10 M. Grouchko, A. Kamyshny, C. F. Mihailescu, D. F. Anghel and S. Magdassi, *ACS Nano*, 2011, **5**, 3354–3359.
- 11 S. Magdassi, M. Grouchko, O. Berezin and A. Kamyshny, *ACS Nano*, 2010, **4**, 1943–1948.
- 12 Y. Tsunomura, Y. Yoshimine, M. Taguchi, T. Baba, T. Kinoshita, H. Kanno, H. Sakata, E. Maruyama and M. Tanaka, *Sol. Energy Mater. Sol. Cells*, 2009, **93**, 670–673.